Research Article
Experimental and Translational Hepatology

JOURNAL
OF HEPATOLOGY

Targeting NAE1-mediated protein hyper-NEDDylation halts cholangiocarcinogenesis and impacts on tumor-stroma crosstalk in experimental models

Graphical abstract

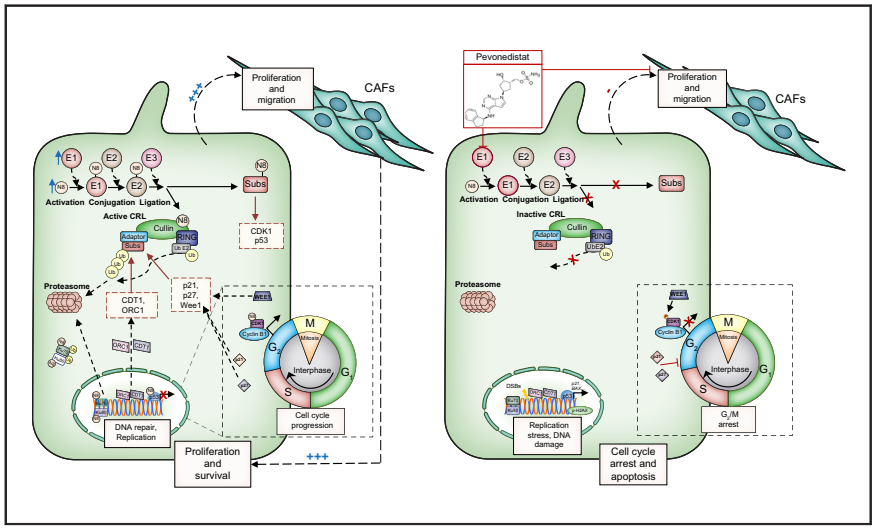

Highlights

- NAE1-dependent protein NEDDylation is increased in human cholangiocarcinoma.
- NEDDylation contributes to cholangiocarcinogenesis favoring pro-survival mechanisms.
- Abnormal NEDDylation alters the cholangiocarcinoma secretome, impacting on the stroma crosstalk.
- Molecular and pharmacological targeting of NAE1 halts experimental tumor growth.
- NAE1 inhibition with pevonedistat is a promising therapy for patients with cholangiocarcinoma.

Authors

Paula Olaizola, Pui Yuen Lee-Law, Maite G. Fernandez-Barrena, …, Pedro M. Rodrigues, Maria J. Perugorria, Jesus M. Banales

Correspondence

jesus.banales@biodonostia.org (J.M. Banales), matxus.perugorria@biodonostia.org (M.J. Perugorria), pedro.rodrigues@biodonostia.org (P.M. Rodrigues).

Lay summary

Little is known about the role of post-translational modifications of proteins in cholangiocarcinoma development and progression. Herein, we show that protein NEDDylation is upregulated and hyperactivated in cholangiocarcinoma, promoting tumor growth. Pharmacological inhibition of NEDDylation halts cholangiocarcinogenesis and could be an effective therapeutic strategy to tackle these tumors.

https://doi.org/10.1016/j.jhep.2022.02.007
 J. Hepatol. 2022, 77, 177–190

Research Article
Experimental and Translational Hepatology

JOURNAL OF HEPATOLOGY

Targeting NAE1-mediated protein hyper-NEDDylation halts cholangiocarcinogenesis and impacts on tumor-stroma crosstalk in experimental models

Paula Olaizola[1], Pui Yuen Lee-Law[1,2], Maite G. Fernandez-Barrena[3,4,5], Laura Alvarez[4], Massimiliano Cadamuro[6], Mikel Azkargorta[3,7], Colm J. O'Rourke[8], Francisco J. Caballero-Camino[1], Irene Olaizola[1], Rocio I.R. Macias[3,9], Jose J.G. Marin[3,9], Marina Serrano-Maciá[10], Maria L. Martinez-Chantar[3,10], Matias A. Avila[3,4,5], Patricia Aspichueta[3,11,12], Diego F. Calvisi[13], Matthias Evert[13], Luca Fabris[6,14], Rui E. Castro[15], Felix Elortza[3,7], Jesper B. Andersen[8], Luis Bujanda[1,3], Pedro M. Rodrigues[1,3,16,*,†], Maria J. Perugorria[1,3,17,*,†], Jesus M. Banales[1,3,16,18,*,†]

[1]*Department of Liver and Gastrointestinal Diseases, Biodonostia Health Research Institute – Donostia University Hospital –, University of the Basque Country (UPV/EHU), San Sebastian, Spain;* [2]*Department of Gastroenterology & Hepatology, Radboud University Nijmegen Medical Center, The Netherlands;* [3]*National Institute for the Study of Liver and Gastrointestinal Diseases (CIBERehd, "Instituto de Salud Carlos III"), Spain;* [4]*Hepatology Program, CIMA. University of Navarra, Pamplona, Spain;* [5]*Instituto de Investigaciones Sanitarias de Navarra (IdiSNA), Pamplona, Spain;* [6]*Department of Molecular Medicine (DMM), University of Padua, Padua, Italy;* [7]*Proteomics Platform, CIC bioGUNE, Basque Research and Technology Alliance (BRTA), ProteoRed-ISCIII, Bizkaia Science and Technology Park, Derio, Spain;* [8]*Biotech Research and Innovation Centre (BRIC), Department of Health and Medical Sciences, University of Copenhagen, Copenhagen, Denmark;* [9]*Experimental Hepatology and Drug Targeting (HEVEPHARM) Group, Institute of Biomedical Research of Salamanca (IBSAL), University of Salamanca, Salamanca, Spain;* [10]*Liver Disease Laboratory, CIC bioGUNE, Basque Research and Technology Alliance (BRTA), Spain;* [11]*Department of Physiology, Faculty of Medicine and Nursing, University of the Basque Country (UPV/EHU), 48940 Leioa, Spain;* [12]*Biocruces Bizkaia Health Research Institute, Cruces University Hospital, 48903 Barakaldo, Spain;* [13]*Institute of Pathology, University of Regensburg, Regensburg, Germany;* [14]*Department of Internal Medicine, Yale Liver Center (YLC), School of Medicine, Yale University New Haven, CT, USA;* [15]*Research Institute for Medicines (iMed.ULisboa), Faculty of Pharmacy, Universidade de Lisboa, Lisbon, Portugal;* [16]*IKERBASQUE, Basque Foundation for Science, Bilbao, Spain;* [17]*Department of Medicine, Faculty of Medicine and Nursing, University of the Basque Country (UPV/EHU), 48940 Leioa, Spain;* [18]*Department of Biochemistry and Genetics, School of Sciences, University of Navarra, Pamplona, Spain*

See Editorial, pages 12–14

Background & Aims: Cholangiocarcinoma (CCA) comprises a heterogeneous group of malignant tumors associated with dismal prognosis. Alterations in post-translational modifications (PTMs), including NEDDylation, result in abnormal protein dynamics, cell disturbances and disease. Herein, we investigate the role of NEDDylation in CCA development and progression.

Methods: Levels and functions of NEDDylation, together with response to pevonedistat (NEDDylation inhibitor) or CRISPR/Cas9 against *NAE1* were evaluated *in vitro*, *in vivo* and/or in patients with CCA. The development of preneoplastic lesions in *Nae1*$^{+/-}$ mice was investigated using an oncogene-driven CCA model. The impact of NEDDylation in CCA cells on tumor-stroma crosstalk was assessed using CCA-derived cancer-associated fibroblasts (CAFs). Proteomic analyses were carried out by mass-spectrometry.

Results: The NEDDylation machinery was found overexpressed and overactivated in human CCA cells and tumors. Most NEDDylated proteins found upregulated in CCA cells, after NEDD8-immunoprecipitation and further proteomics, participate in the cell cycle, proliferation or survival. Genetic (CRISPR/Cas9-*NAE1*) and pharmacological (pevonedistat) inhibition of NEDDylation reduced CCA cell proliferation and impeded colony formation *in vitro*. NEDDylation depletion (pevonedistat or *Nae1*$^{+/-}$ mice) halted tumorigenesis in subcutaneous, orthotopic, and oncogene-driven models of CCA *in vivo*. Moreover, pevonedistat potentiated chemotherapy-induced cell death in CCA cells *in vitro*. Mechanistically, impaired NEDDylation triggered the accumulation of both cullin RING ligase and NEDD8 substrates, inducing DNA damage and cell cycle arrest. Furthermore, impaired NEDDylation in CCA cells reduced the secretion of proteins involved in fibroblast activation, angiogenesis, and oncogenic pathways, ultimately hampering CAF proliferation and migration.

Conclusion: Aberrant protein NEDDylation contributes to cholangiocarcinogenesis by promoting cell survival and proliferation. Moreover, NEDDylation impacts the CCA-stroma crosstalk. Inhibition of NEDDylation with pevonedistat may represent a potential therapeutic strategy for patients with CCA.

Keywords: Cholangiocarcinoma; protein NEDDylation; pathogenesis; tumor microenvironment; therapy.
Received 15 June 2021; received in revised form 13 January 2022; accepted 8 February 2022; available online 23 February 2022
* Corresponding authors. Address: Department of Liver and Gastrointestinal Diseases, Biodonostia Health Research Institute – Donostia University Hospital, Paseo del Dr. Begiristain s/n, E-20014, San Sebastian, Spain; Tel.: +34 943006067.
E-mail addresses: jesus.banales@biodonostia.org (J.M. Banales) matxus.perugorria@biodonostia.org (M.J. Perugorria) pedro.rodrigues@biodonostia.org (P.M. Rodrigues)
† Share senior authorship
https://doi.org/10.1016/j.jhep.2022.02.007

Lay summary: Little is known about the role of post-translational modifications of proteins in cholangiocarcinoma development and progression. Herein, we show that protein NEDDylation is upregulated and hyperactivated in cholangiocarcinoma, promoting tumor growth. Pharmacological inhibition of NEDDylation halts cholangiocarcinogenesis and could be an effective therapeutic strategy to tackle these tumors.

Introduction

Cholangiocarcinoma (CCA) comprises a heterogeneous group of malignancies emerging at every point of the biliary tree.[1] According to their anatomical location, CCAs are classified as intrahepatic (iCCA), perihilar, or distal, displaying different clinicopathological and molecular features.[1] The incidence of these tumors (~5:100,000) is rising globally, becoming a major health and social problem.[1] CCA is generally asymptomatic in early stages and, consequently, commonly diagnosed at advanced phases when symptoms associated with biliary obstruction arise. This situation severely compromises the access to potential curative options, mainly based on surgery.[1] Moreover, the high risk of tumor recurrence and the elevated chemoresistance of CCAs contribute to patients' poor prognosis.

From a molecular point of view, CCAs are highly heterogeneous, with different genetic, epigenetic, and cell signaling abnormalities.[2] These tumors are characterized by a highly desmoplastic tumor microenvironment (TME), prevalently composed of cancer-associated fibroblasts (CAFs) that produce extracellular matrix components, and of inflammatory cells and endothelial cells, which interact with each other to promote the neoplastic transformation of the cells lining the bile ducts (*i.e.*, cholangiocytes) and tumor progression.[3] Given the complex biology of CCA, it is fundamental to identify key, and if possible cross-sectional, molecular mechanisms involved in cholangiocarcinogenesis. Interaction between transcriptional, post-transcriptional and post-translational regulation is a subject of cutting-edge research, as cells must respond immediately to changes in the microenvironment to maintain homeostasis and activate alternative mechanisms.

Post-translational modifications (PTMs) are highly dynamic and often reversible processes whereby a protein or a chemical group binds to another protein. These chemical changes alter the structure and properties of individual proteins, affecting their activity, stability, and localization.[4] PTMs, which include phosphorylation, glycosylation, ubiquitination, SUMOylation, NEDDylation, disulfide bonding, acetylation, lipidation, methylation, and hydroxylation, provide rapid mechanisms for the activation or inhibition of signaling pathways and metabolism of proteins. Given their relevance in physiological processes, perturbation of PTMs commonly leads to cell disturbances and disease. Among the variety of PTMs that can participate in the pathogenesis of diseases, NEDDylation has recently been described and is still poorly understood, although it seems to regulate a wide range of cellular processes considered relevant for cancer.

Protein NEDDylation results from the covalent and reversible attachment of NEDD8 to a lysine residue of the substrate protein.[5] NEDD8 binding to proteins is catalyzed by a 3-step enzymatic cascade that involves the heterodimer NEDD8-activating enzyme E1 (NAE, which comprises the NAE regulatory subunit [NAE1] and the ubiquitin-activating enzyme 3 [UBA3]), NEDD8 conjugating E2 enzymes (ubiquitin-conjugating enzyme E2F [UBE2F] and E2M [UBE2M]) and substrate-specific E3 ligases. The best characterized substrate of NEDD8 is the cullin family of proteins. Cullins act as a molecular scaffold, together with an adaptor protein, a substrate acceptor, and a RING protein to form the cullin RING ligases (CRLs), well-known E3 ubiquitin ligases. Increased protein NEDDylation has already been reported in several human diseases.[6,7] Notably, pevonedistat, a first-in-class selective NAE inhibitor has been developed, leading to the accumulation of CRL substrates and destabilization of certain oncoproteins, ultimately hindering increased cell growth.[8] Therefore, we herein aimed to explore in detail the role of NEDDylation in cholangiocarcinogenesis and evaluate the therapeutic potential of pevonedistat in experimental models of CCA.

Material and methods

Human samples

CCA and surrounding control tissues (liver or normal bile ducts) from 7 independent cohorts of patients (Copenhagen [Denmark; GSE26566], The Cancer Genome Atlas [TCGA], The Thailand Initiative in Genomics and Expression Research [TIGER-LC; GSE76311], Job [E-MTAB-6389], Regensburg [Germany; #17-1015-101], Nakamura [EGA00001000950] and Jusakul [GEO: GSE89749]) were studied at transcriptomic level. Immunohistochemistry (IHC) was performed in paraffin-embedded iCCA tissues from the Institute of Pathology at University of Regensburg. The research protocol was approved by the Clinical Research Ethic Committee from the Medical University of Regensburg (Germany, #17-1015-101), and all patients signed written consents to allow the use of their samples for biomedical research.

Cell cultures

Normal human cholangiocytes (NHCs) were isolated from normal liver tissue. Five human CCA cell lines were employed: HUCCT1, TKKK (both iCCA), EGI1, TFK1, and WITT (all 3 extrahepatic CCAs). CAFs were isolated from resected iCCAs at the Ospedale di Padova (Italy) and at Biodonostia Health Research Institute (Spain). Cell isolation, culture and characterization are described in the supplementary information.

RNA isolation and gene expression

Total RNA was isolated from both human liver samples (*i.e.*, CCA tumors and surrounding normal liver tissue) and cells in culture using the TRI Reagent®, following the manufacturer's instructions. Subsequently, reverse transcription and quantitative real-time PCR were conducted as described in the supplementary information. Primer sequences (Sigma) are reported in Table S1.

Histological analyses

H&E staining was performed to analyze tissue morphology as previously described.[9] Detection of NAE1 and NEDD8 protein expression (*i.e.*, free NEDD8 and NEDD8-conjugated proteins) by IHC was carried out on paraffin-embedded sections from normal surrounding, biliary intra-epithelial neoplasia (BilIN), and CCA human liver tissue, as previously described.[10] Proliferating cell nuclear antigen (PCNA) was detected by IHC in subcutaneous CCA tumors as previously described.[9] Antibodies are listed in Table S2.

Immunoblotting
Changes in protein expression were analyzed by immunoblotting using whole cell lysates or NEDD8-immunoprecipitation (IP) cell lysates of cultured NHC, CCA cells, CAFs and/or LX2, as described in the supplementary information. Protein NEDDylation levels were measured in CCA cells in the presence of increasing concentrations of VEGF, EGF, IL-6 and Wnt3a. The antibodies used are listed in Table S2.

Immunofluorescence
DNA damage and DNA repair dynamics induced by pevonedistat (0.3 μM) and/or cisplatin (10 μM) were analyzed by immunofluorescence of phosphorylated-histone 2A family member X (p-H2AX) as described in the supplementary information. Ki67 and cleaved caspase-3 were detected by immunofluorescence in CCA tumors from subcutaneous as indicated in the supplementary information.

Cell viability, proliferation, cell cycle, and apoptosis
Cell viability, proliferation, cell cycle, and apoptosis assays in normal and tumor cholangiocytes were evaluated in the presence or absence of pevonedistat at different concentrations (0.1-1 μM) for 72 hours or Ro-3306 (9 μM) for 24 hours, as described in the supplementary information. In addition, CAF viability was assessed in the presence of pevonedistat, and CAF and CCA cell proliferation were determined in the presence or absence of conditioned media from CAFs or CCA cells.

Hanging droplet spheroids
3D spheroids were generated through the hanging droplet method and monitored in the presence or absence of pevonedistat (0.3 μM) for 72 hours. Details are outlined in the supplementary information.

Colony formation
Colony formation capacity was explored by *in vitro* seeding EGI1 or HUCCT1 cells into agar-coated 6-well plates and culturing them with pevonedistat (0.3 μM) or vehicle (DMSO) for 3 weeks. Detailed culturing information is provided in the supplementary information.

Cell migration
Cell migration was evaluated *in vitro* with "wound-healing" assays, as described in the supplementary information.

CRISPR/Cas9
NAE1 was knocked-down by CRISPR/Cas9 methodology in CCA cells as described in the supplementary information.

Reactive oxygen species detection
Intracellular reactive oxygen species were measured using the CellROX™ Deep Red Reagent in CRISPR/Cas9 control and *NAE1*-knockdown CCA cells following the manufacturer's instructions, as detailed in the supplementary information.

Immunoprecipitation
Whole cell lysates from NHC and CCA cells (EGI1) were incubated with Dynabeads Protein G, which were crosslinked to NEDD8 or IgG antibodies. Proteins were eluted from the beads with 2% sodium dodecyl sulfate, as described in the supplementary information.

Mass-spectrometry and proteomic analysis
Comparative shotgun proteomic analyses of NEDD8-IP, as well as CRISPR control and *NAE1*-knockdown EGI1 clone lysates were performed as described in the supplementary information.

Experimental animal models of CCA
Xenograft, orthotopic and oncogene-driven CCA models were generated and employed as described in the supplementary information.

Statistical analysis
Statistical analyses were performed as described in the supplementary information.

Results
The NEDDylation machinery is upregulated in CCA
To evaluate whether NEDDylation was dysregulated in CCA, the expression of the activating enzyme *NAE1* and the ligand *NEDD8*, was analyzed in human resected CCA and control tissues (*i.e.*, surrounding liver or normal bile ducts) in 5 different cohorts of patients (*i.e.*, Copenhagen, TCGA, TIGER-LC, Job and Regensburg). *NAE1* and *NEDD8* mRNA expression was consistently increased in CCA tumor samples from all independent cohorts compared to both controls (Fig. 1A). Notably, their expression was found upregulated in resected CCA tissues from the Copenhagen and Nakamura cohorts independently of underlying mutations (*IDH1*, *KRAS*, *TP53*, or wild-type status for all 3 genes) (Fig. S1A), altogether pinpointing the upregulation of the NEDDylation machinery as a common event in CCA. Interestingly, *NAE1* upregulation was not associated with changes in gene promoter methylation status (Fig. S1B). Furthermore, moderate/poorly-differentiated tumors from the Copenhagen cohort were characterized by higher *NAE1* expression compared to well-differentiated ones (Fig. 1B). Laser microdissection studies on CCA tumor samples from the Copenhagen cohort revealed increased *NAE1* expression in CCA epithelia compared to matched tumor stroma (mainly formed by CAFs, immune cells such as tumor-associated macrophages, and endothelial cells) (Fig. 1C). In contrast, no correlation was found between *NAE1* expression and tumor size, perineural invasion, lymph node invasion or metastasis (Fig. S2A-C). Patients with high tumor levels of *NAE1* or *NEDD8* displayed a tendency to present worse overall survival compared to patients with low *NAE1* or *NEDD8* levels (Fig. S2D). Regarding CCA subtypes, *NAE1* or *NEDD8* expression variability was observed depending on the cohort analyzed (supplementary information and Fig. S3).

NAE1 and NEDD8 (*i.e.*, the combination of free and protein-conjugated) protein levels were evaluated in different disease states within the Regensburg cohort (*i.e.*, pre-invasive lesions, such as BilIN, and iCCAs with distinct differentiation grades [G1 and G3]) by IHC. Immunoreactivity for NAE1 and NEDD8 was almost absent in non-tumorous tissues, while similarly strong nuclear and/or cytoplasmic immunoreactivity for NAE1 and NEDD8 proteins was detected in pre-invasive lesions, as well as in G1 and G3 iCCAs. These results demonstrate that increased levels of NAE1 and NEDD8 are a general phenomenon in CCA, being already evident in pre-malignant states (Fig. 1D).

To determine whether NEDDylation was also altered at cellular level, the same array of genes was analyzed in 5 human CCA cell lines (*i.e.*, HUCCT1, EGI1, TFK1, WITT and TKKK) compared to NHC. *NAE1* was found overexpressed in all CCA cell lines compared to NHCs, corroborating the results obtained in

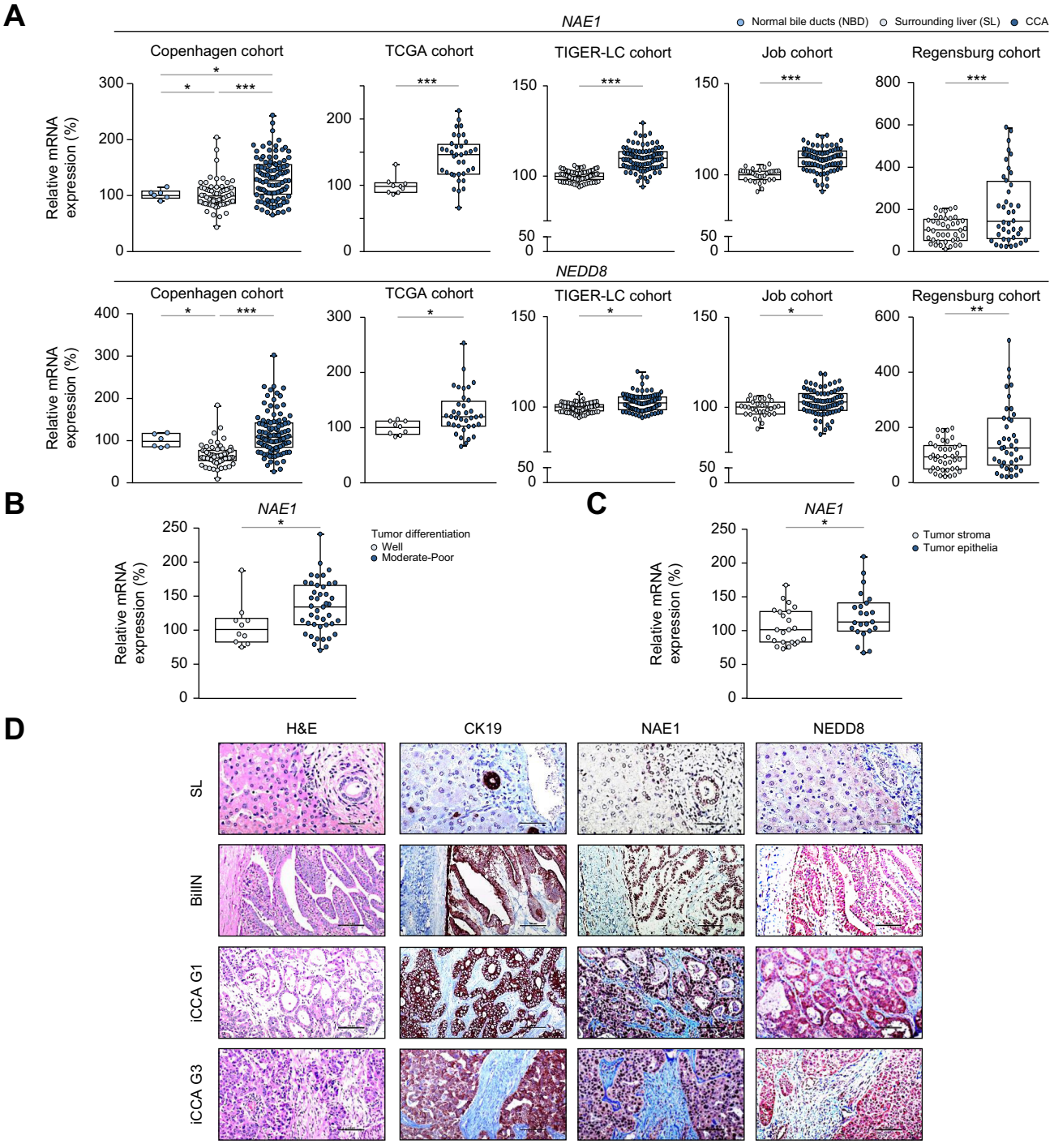

Fig. 1. Expression levels of the NEDDylation pathway components in human CCA tissue. (A) *NAE1* and *NEDD8* mRNA expression in CCA tumors compared to NBDs and/or surrounding human liver tissue from the Copenhagen, TCGA, TIGER-LC, Job, and Regensburg cohorts of patients. (B) *NAE1* mRNA expression in CCA tumors from the Copenhagen cohort grouped by tumor differentiation grade and (C) compared to matched tumor stroma tissue. (D) NAE1 and NEDD8 (free and protein-conjugated) expression in human non-tumorous SL, BilIN and iCCA of different differentiation grades. CK19 staining was used as biliary marker. 400x in SL; scale bar 50 μm; 200x in BilIN, iCCA G1 and G3; scale bar 100 μm. *p <0.05; ***p <0.001 (Kruskal-Wallis, Mann-Whitney and paired/unpaired Student's t tests). BilIN, biliary intra-epithelial neoplasia; CCA, cholangiocarcinoma; CK19, cytokeratin 19; iCCA, intrahepatic cholangiocarcinoma; NBDs, normal bile ducts; SL, surrounding liver; TCGA, The Cancer Genome Atlas; TIGER-LC, The Thailand Initiative in Genomics and Expression Research.

human tissue (Fig. 2A). Regarding *NEDD8* expression, no significant differences were observed between CCA cells and NHCs, except for TKKK cells (Fig. 2A). Importantly, increased levels of NEDD8-conjugated proteins were found in all CCA cell lines compared to NHCs by immunoblot (Fig. 2B), while such an increase was not observed for free NEDD8 (Fig. 2B).

In order to understand the potential mechanisms behind the upregulation of the NEDDylation pathway in CCA, the role of

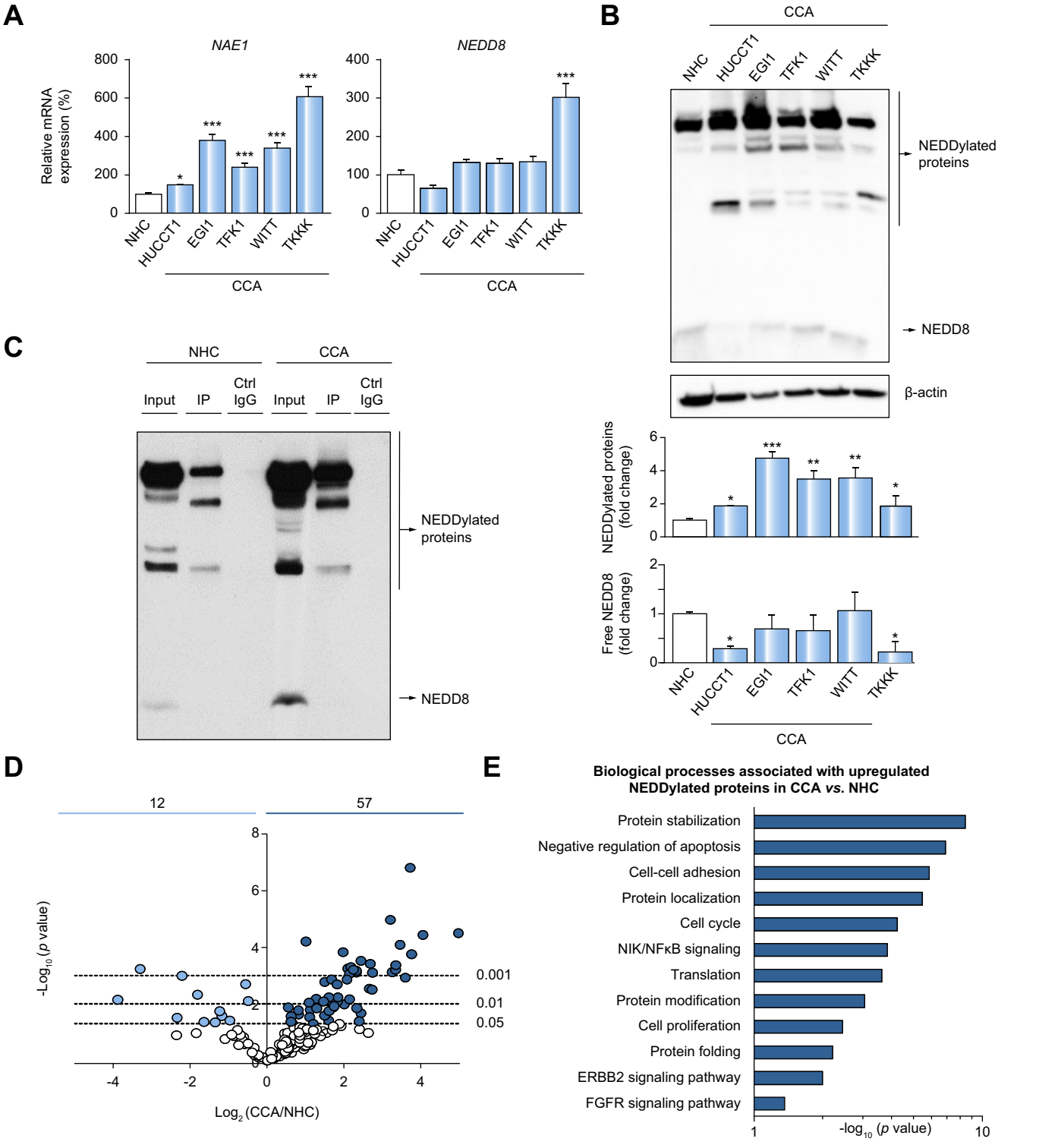

Fig. 2. Aberrant expression of NEDDylation pathway components in human CCA cells *in vitro*. (A) *NAE1* and *NEDD8* mRNA expression in NHCs and CCA cell lines (n = 6). (B) Representative immunoblot and quantification of NEDD8 and NEDD8-conjugated proteins in NHCs and CCA cells (n = 6). (C) Representative immunoblot of NEDD8-IP in NHCs and CCA (EGI1) cells (n = 3). (D) Volcano plot of all identified NEDD8-IP proteins (n = 240) by mass-spectrometry comparing fold enrichment in CCA cells to NHCs. (E) Proteomic analyses of significant identified proteins (n = 69) between CCA cells and NHCs by GO. **p* <0.05; ****p* <0.001 (Student's or Mann-Whitney *t* tests). CCA, cholangiocarcinoma; Ctrl, control; IP, immunoprecipitation; NHCs, normal human cholangiocytes.

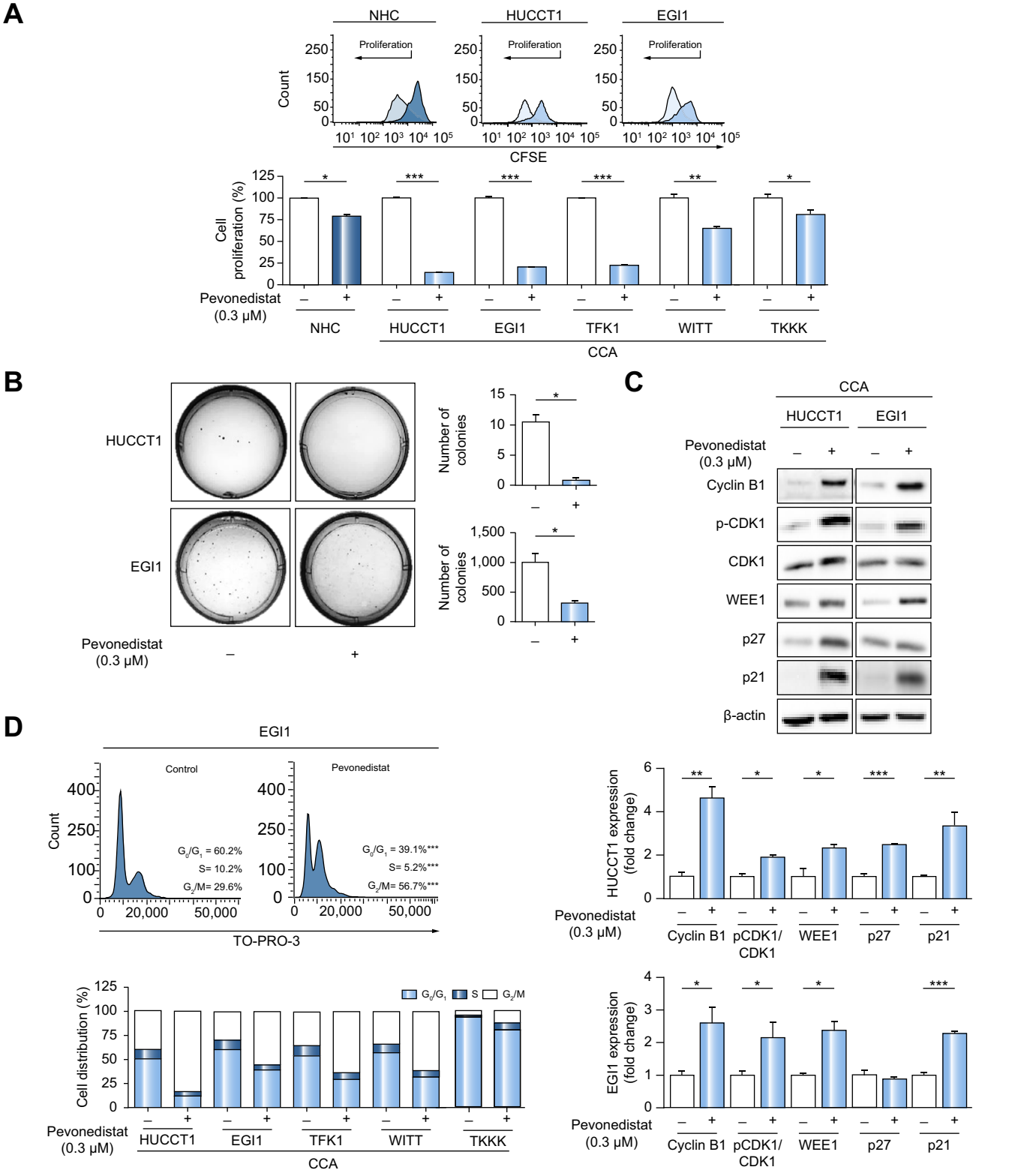

Fig. 3. Pevonedistat induces cell cycle arrest, hindering proliferation and colony growth of CCA cells in culture. (A) Cell proliferation in NHCs and CCA cell lines after incubation with pevonedistat (n = 6). (B) Soft agar colony formation assays in HUCCT1 and EGI1 CCA cells in the presence or absence of pevonedistat (n = 6). (C) Representative immunoblot and quantification of cyclin B1, p-CDK1, CDK1, WEE1, p27, and p21 in HUCCT1 and EGI1 CCA cells in the presence or absence of pevonedistat (n = 3). (D) Cell cycle in CCA cells in the presence or absence of pevonedistat (n = 6). $^{*}p$ <0.05, $^{**}p$ <0.01, $^{***}p$ <0.001 (Mann-Whitney or Student's *t* tests). CCA, cholangiocarcinoma; NHCs, normal human cholangiocytes.

different ligands involved in cholangiocarcinogenesis (VEGF, EGF, IL-6 and Wnt3a) was further evaluated on NEDD8-conjugation in HUCCT1 and EGI1 cells. Immunoblotting analysis showed that protein NEDDylation is upregulated by VEGF in EGI1 cells and by IL-6 in HUCCT1 cells (Fig. S4), suggesting that angiogenic and inflammatory factors might be involved in the regulation of the NEDDylation pathway in CCA.

Increased NEDDylated proteins contribute to cholangiocarcinogenesis

To identify the NEDDylation targets that could underlie cholangiocarcinogenesis, NEDD8-conjugated proteins were isolated from CCA cell lines and NHCs after IP and analyzed by mass-spectrometry. Immunoblotting confirmed enrichment of NEDD8-IP proteins compared to controls (inputs or control IgG) in respective cell cultures (Fig. 2C). Shotgun proteomic analysis identified 69 differentially NEDDylated proteins between CCA cells (EGI1) and NHCs. Specifically, the levels of 57 proteins (83%) were increased (dark blue), while those of 12 proteins (17%) decreased (light blue) in CCA cells compared to NHCs (Fig. 2D). Gene ontology (GO) analysis of the NEDDylated proteins found upregulated in CCA revealed that they participate in biological processes related to protein stabilization (*i.e.*, HSP90AA1, HSPA1A, CCT3), localization (*i.e.*, KPNA2, RAN) as well as to survival (*i.e.*, p53), cell cycle (*i.e.*, p53, CDK1), DNA repair (*i.e.*, XRCC5, XRCC6), and proliferation (*i.e.*, PRKDC, PHB) (Fig. 2E). Notably, several proteins of the NEDDylation pathway (*i.e.*, NAE1, UBA3, UBE2M) were found hyper-NEDDylated in EGI1 compared to NHCs, supporting the increased activity of the pathway in CCA cell lines. Moreover, the proteomic analysis identified increased NEDDylated levels of cullins 1-3, 4A, and 5 in EGI1 cells compared to NHCs. Further immunoblotting analysis including all 5 CCA cell lines indicated that CUL-1, 4A and 5 are generally found upregulated in almost all of them, when compared with NHCs (Fig. S5).

Pevonedistat induces DNA damage and cell cycle arrest, repressing CCA cell proliferation and inducing apoptosis

Considering the hyper-NEDDylation status of CCA cells and its potential involvement in cholangiocarcinogenesis, we next evaluated the effect of pevonedistat on CCA. Pevonedistat reduced the levels of NEDD8-conjugated proteins in all CCA cell lines, as well as in NHCs, in a dose-dependent manner (Fig. S6). Moreover, pharmacological inhibition of NEDDylation resulted in decreased cell viability of all CCA cell lines in a dose-dependent manner, whereas NHC viability remained unaffected (Fig. S7A). In this regard, the aberrant proliferation of CCA cells and their ability to form anchorage-independent colonies were reduced after incubation with pevonedistat (Fig. 3A,B; Fig. S7B). As expected, pevonedistat triggered the accumulation of CRL substrates –including cell cycle inhibitors such as p21, p27, and WEE1 – as well as the increment of the G_2 phase marker cyclin B1 in CCA cells (Fig. 3C); moreover, the p-CDK1/CDK1 ratio in CCA cells was increased, altogether indicating that pevonedistat induced cell cycle arrest in the G_2/M phase in CCA (Fig. 3C,D and Fig. S7C). Of note, the exposure of CCA cells to a selective inhibitor of the CDK1/cyclin B1 axis (Ro-3306) also resulted in G_2/M cell cycle arrest (Fig. S8A), highlighting the relevance of this complex in CCA.

Cell cycle arrest in G_2/M is regulated by the G_2/M DNA damage checkpoint, which prevents mitosis initiation until damaged or incompletely replicated DNA is sufficiently repaired. Thus, we next studied whether pevonedistat could induce DNA replication stress or damage and, therefore, activate this checkpoint and arrest the cell cycle. For this purpose, we evaluated the abundance of CDT1 and ORC1, well-known substrates of CRLs involved in DNA replication. Administration of pevonedistat induced the accumulation of CDT1 and ORC1 (Fig. 4A), which could cause replicative stress and DNA damage. Indeed, immunoblotting and immunofluorescence revealed a noticeable increase of the DNA damage marker p-H2AX upon pevonedistat incubation (Fig. 4A,B) and DNA damage response activation in CCA cells (Fig. S8B). In contrast to cisplatin, pevonedistat generated unrepairable DNA damage (Fig. S9). Notably, the triple combination of pevonedistat and gemcitabine/cisplatin (GemCis), standard of care palliative chemotherapy for patients with unresectable CCA,[1] reduced CCA cell viability compared to GemCis, each drug alone, or untreated cells (Fig. 4C).

The expression of several apoptotic markers (*i.e.*, *BAK*, *BAX*, *BIM*, and *NOXA*) was upregulated upon pevonedistat (Fig. S10A). In agreement, pevonedistat increased cell death in both normal and tumor cholangiocytes, with a milder effect in NHCs (Fig. 4D, Fig. S10B). Additionally, incubation of 3D CCA (EGI1) spheroids with pevonedistat caused spheroid shrinkage, while no differences were observed in 3D NHC spheroid cultures (Fig. 4E).

Pevonedistat halts CCA growth *in vivo*

Pevonedistat administration halted tumor growth *in vivo*, as shown by the reduction of subcutaneous tumor volume compared to vehicle-treated animals (Fig. 5A-D). Pevonedistat increased cleaved caspase-3 levels in subcutaneous CCA tumors, indicating that tumor shrinkage mainly happens due to apoptosis induction rather than decreased cell proliferation (Fig. 5E, Fig. S11). Moreover, the absence of orthotopic tumor expansion over time, measured by luminescence, was observed in mice receiving pevonedistat (Fig. 5F-I), presenting minimal neoplastic areas in their livers compared to controls that showed increased tumorigenesis (Fig. 5J).

CRISPR/Cas9-mediated *NAE1* knockdown mimics the effects of pevonedistat in CCA *in vitro* and *in vivo*

To compare the effects of pevonedistat, stable CRISPR/Cas9-mediated *NAE1*-knockdown in CCA (EGI1) cells was evaluated. Immunoblotting confirmed *NAE1* silencing, as NAE1 protein levels were reduced by 85% in CRISPR/Cas9-*NAE1* CCA cells compared to CRISPR/Cas9 control or wild-type (Fig. 6A). Consistently, *NAE1*-knockdown CCA cells barely expressed *NAE1* at the mRNA level (Fig. S12A) and exhibited reduced protein NEDDylation (Fig. S12B). Similar to pevonedistat, *NAE1* depletion had an anti-proliferative effect on CCA cells compared to CRISPR/Cas9 control cells (Fig. 6B) with a concomitant accumulation of p21 (Fig. S12C). *NAE1*-knockdown CCA cells were unable to form anchorage-independent colonies or 3D hanging-spheroids (Fig. 6C,D). Importantly, these findings were recapitulated when comparing CRISPR/Cas9 control or wild-type cells with a second *NAE1*-knockdown clone (#2; supplementary information, Table S4 and Fig. S13). The lack of spheroid-forming capacity could be associated with a more differentiated and a less stem-like phenotype. Thus, the expression of the stemness markers *CD133*, *OCT4*, and *SOX2* was downregulated in CRISPR/Cas9-*NAE1* CCA cells (Fig. 6E). Shotgun proteomic analyses identified a total of 781 differentially expressed proteins between CRISPR/Cas9-

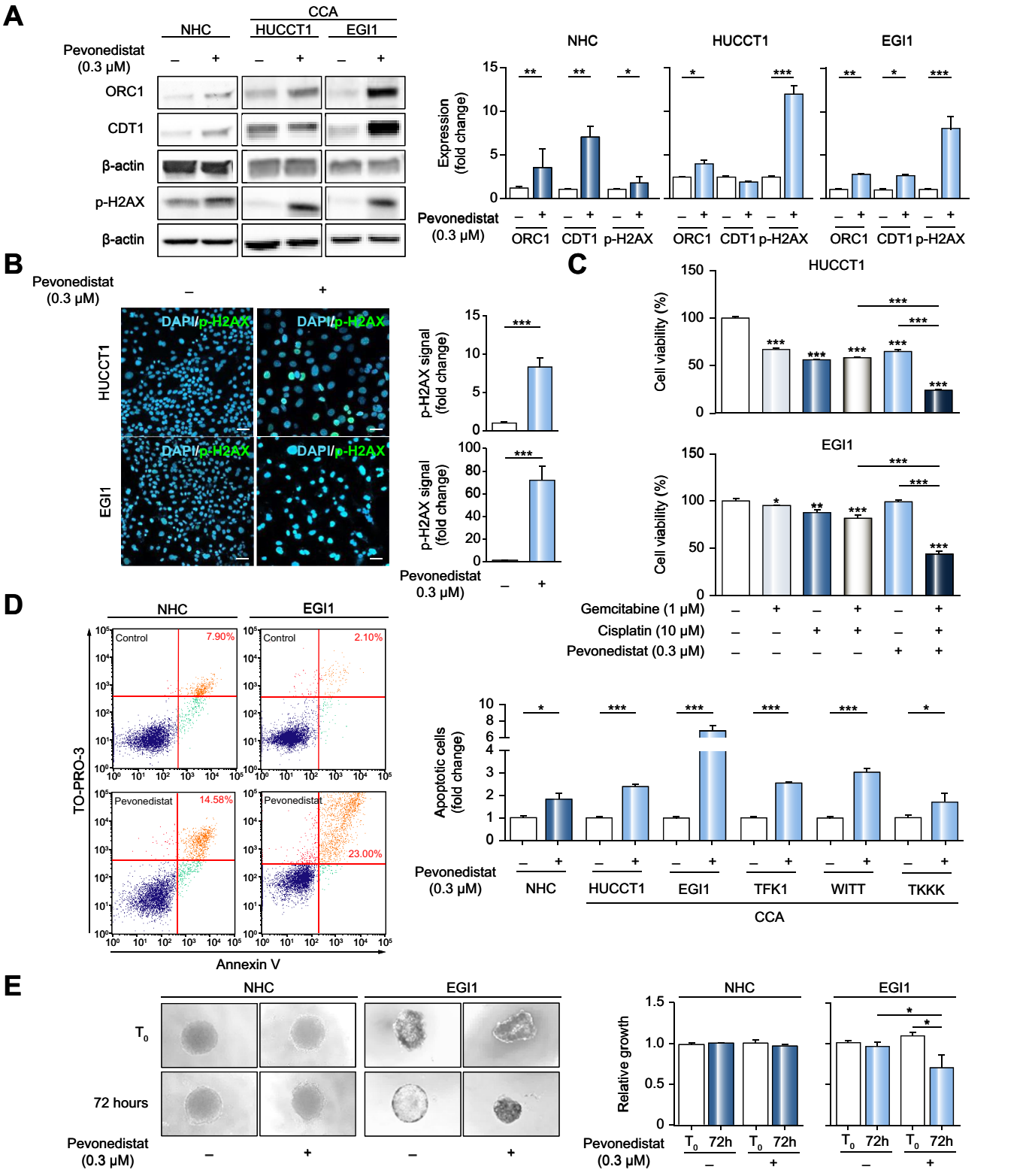

Fig. 4. Pevonedistat induces DNA damage, apoptosis, and sensitizes CCA cells to chemotherapeutic agents. (A) Representative immunoblot and quantification of ORC1, CDT1, and p-H2AX in NHCs, HUCCT1 and EGI1 cells after incubation with pevonedistat (n = 3). (B) Immunofluorescence images and quantification of p-H2AX in HUCCT1 and EGI1 cells in the presence or absence of pevonedistat (n = 15). Scale bar: 20 μm. (C) Cell viability in untreated, gemcitabine- and/or cisplatin- and/or pevonedistat-treated HUCCT1 and EGI1 CCA cell lines (n = 6). (D) Apoptosis of NHCs and CCA cell lines after pevonedistat incubation (n = 6). (E) 3D spheroids of NHCs and EGI1 cells at baseline (T_0) and after incubation with pevonedistat (n = 10). *p <0.05, **p <0.01, ***p <0.001 (one-way ANOVA or Student's t tests). CCA, cholangiocarcinoma; NHCs, normal human cholangiocytes.

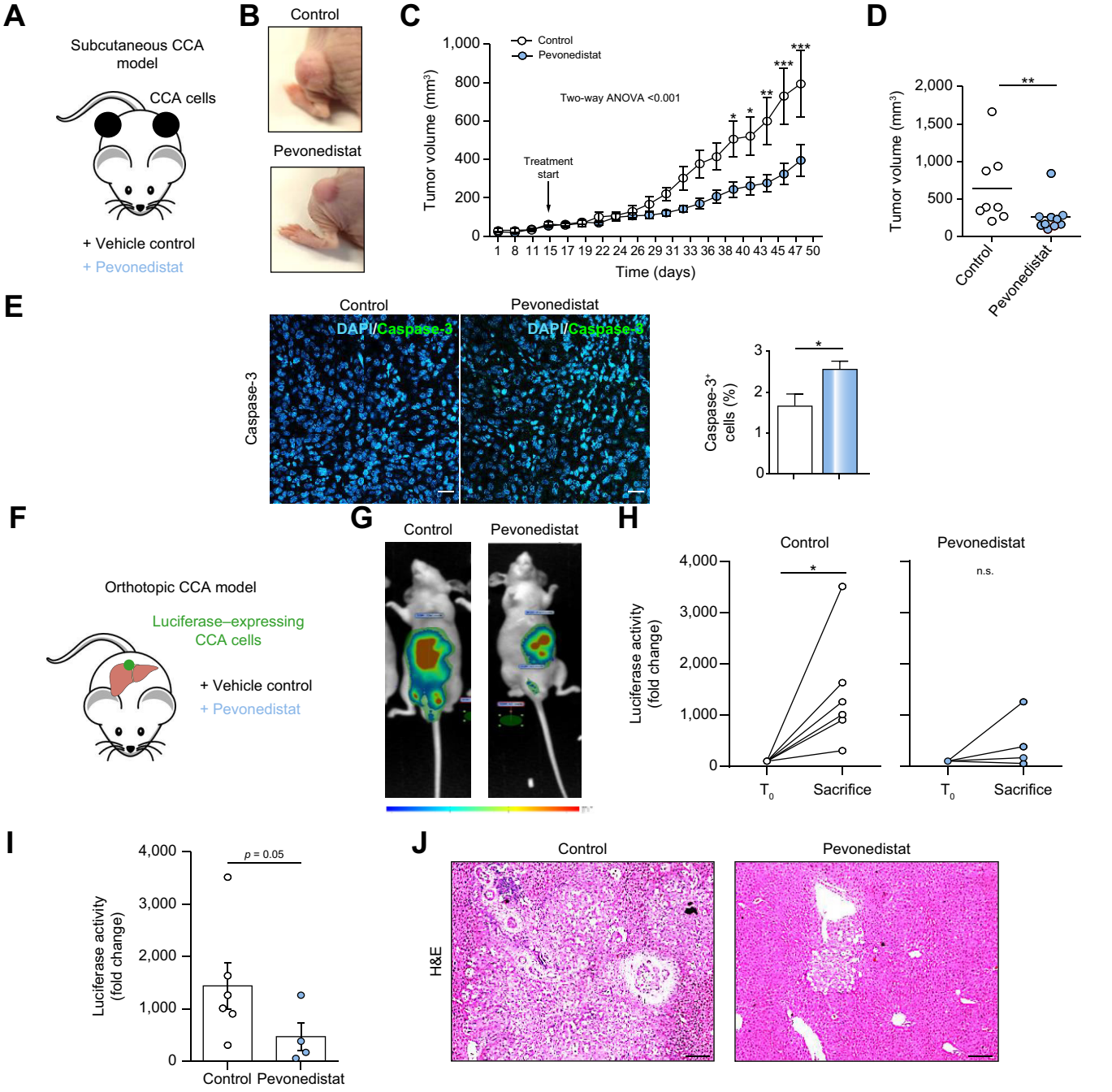

Fig. 5. Pevonedistat halts CCA growth in subcutaneous and orthotopic models of CCA. (A) Subcutaneous CCA model chart. (B) Representative images of vehicle- or pevonedistat-administered CCA tumors. (C) Tumor volume growth and (D) tumor volume of xenografts at sacrifice. (E) Immunofluorescence images and quantification of caspase-3 in subcutaneous CCA tumors exposed or not to pevonedistat. Scale bar: 20 μm. (F) Orthotopic CCA model chart. (G) Representative images of luciferase expression of vehicle (n = 6) or pevonedistat-treated (n = 4) immunodeficient mice harboring orthotopic tumors, (H) quantification at the beginning of treatment (T_0) and at sacrifice, and fold-change of luciferase activity between sacrifice and T_0 timepoints. (J) Representative H&E images of liver lesions of vehicle- and pevonedistat-treated animals. *p <0.05, **p <0.01 (two-way ANOVA, Mann-Whitney or Student's t tests). CCA, cholangiocarcinoma; n.s., non significant.

NAE1 and control CCA cells. Among them, 372 proteins (47.6%) were upregulated (red) and 409 (52.4%) downregulated (blue) in CRISPR/Cas9-*NAE1* CCA cells compared to controls (Fig. S12D). GO analysis revealed that the upregulated proteins in CRISPR/Cas9-*NAE1* CCA cells are involved in different biological processes, including cellular respiration (*e.g.*, NUFA8, UQCRC1), vesicle transport (*e.g.*, SEC22B, VAMP3), negative regulation of MAPKKK pathway (*e.g.*, PEBP1), tricarboxylic (TCA) cycle (*e.g.*, DLST, SUCLA2) and oxidation/reduction activity (*e.g.*, PRDX2, TXN) (Fig. S12E), the latter being supported by increased oxidative stress compared to control cells (Fig. 6F). In contrast, translation (*e.g.*, EIF3E, EIF3F), cell cycle (*e.g.*, PCNA, DMC1), intracellular transport (*e.g.*, COPB1, KIF1C), protein biogenesis, assembly and folding (*e.g.*, CCT3, HSP90AA1), as well as DNA

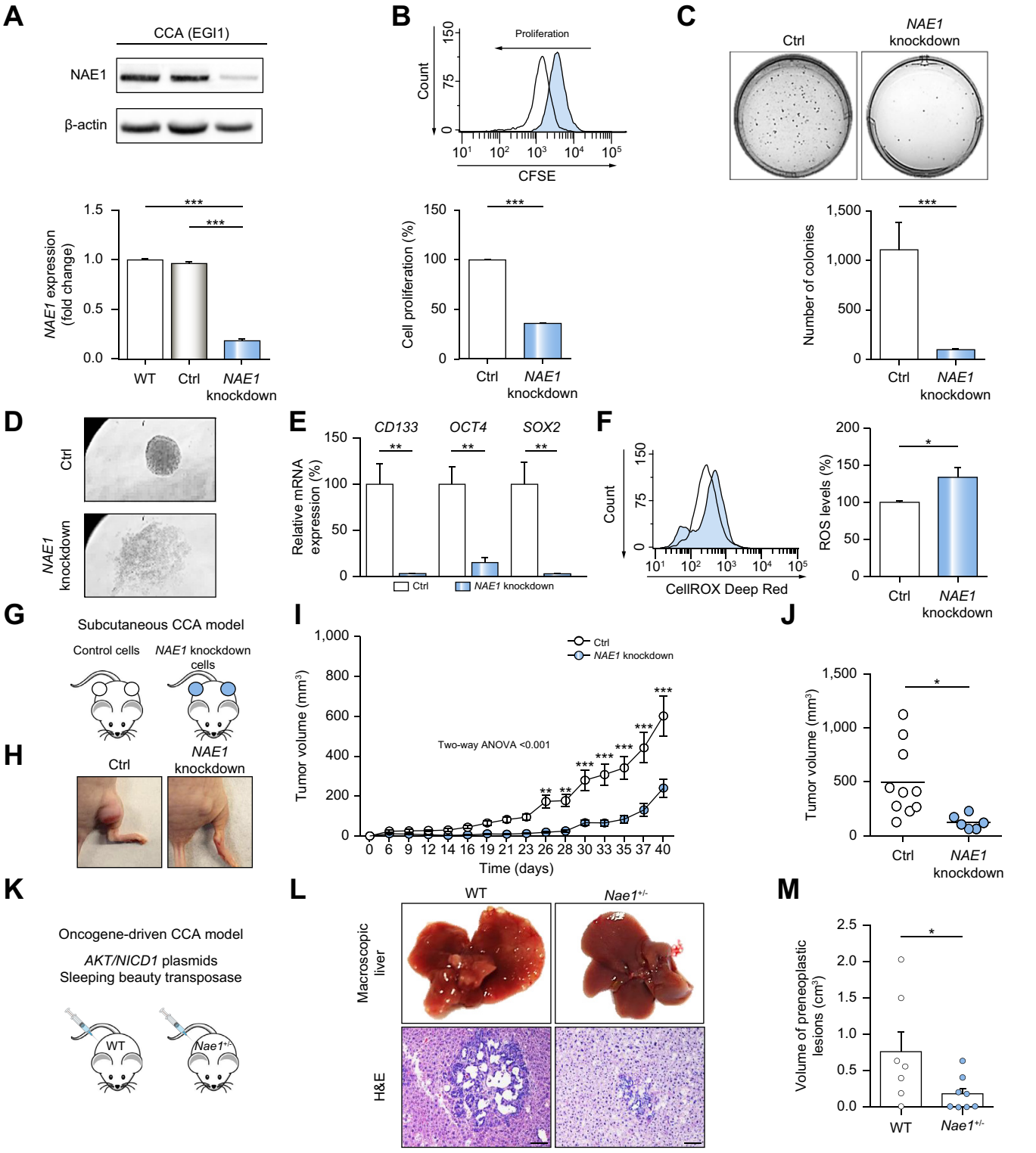

Fig. 6. CRISPR/Cas9-*NAE1* CCA cells recapitulate pevonedistat effects on CCA progression. (A) Representative immunoblot and quantification of WT, CRISPR/Cas9 control (Ctrl), and *NAE1*-knockdown CCA (EGI1) cells (n = 6). (B) Proliferation (n = 3), (C) colony (n = 3) and (D) spheroid formation ability (n = 10), and (E) mRNA expression of stemness markers in Ctrl and *NAE1*-knockdown CCA cells (n = 6). (F) ROS levels in Ctrl and *NAE1*-knockdown CCA cells (n = 3). (G) Subcutaneous CCA model chart with the injection of Ctrl and *NAE*1-knockdown CCA cells. (H) Representative images of the tumors. (I) Tumor volume growth and (J) tumor volume of xenografts at sacrifice. (K) Oncogene-driven CCA model chart in WT (n = 7) and *Nae1*$^{+/-}$ (n = 8) mice. (L) Representative macroscopic images of the livers at sacrifice, H&E staining and (M) quantification of preneoplastic lesions. **p* <0.05, ***p* <0.01, ****p* <0.001 (two-way ANOVA, one-way ANOVA, Mann-Whitney or Student's *t* tests). CCA, cholangiocarcinoma; Ctrl, control; ROS, reactive oxygen species; WT, wild-type.

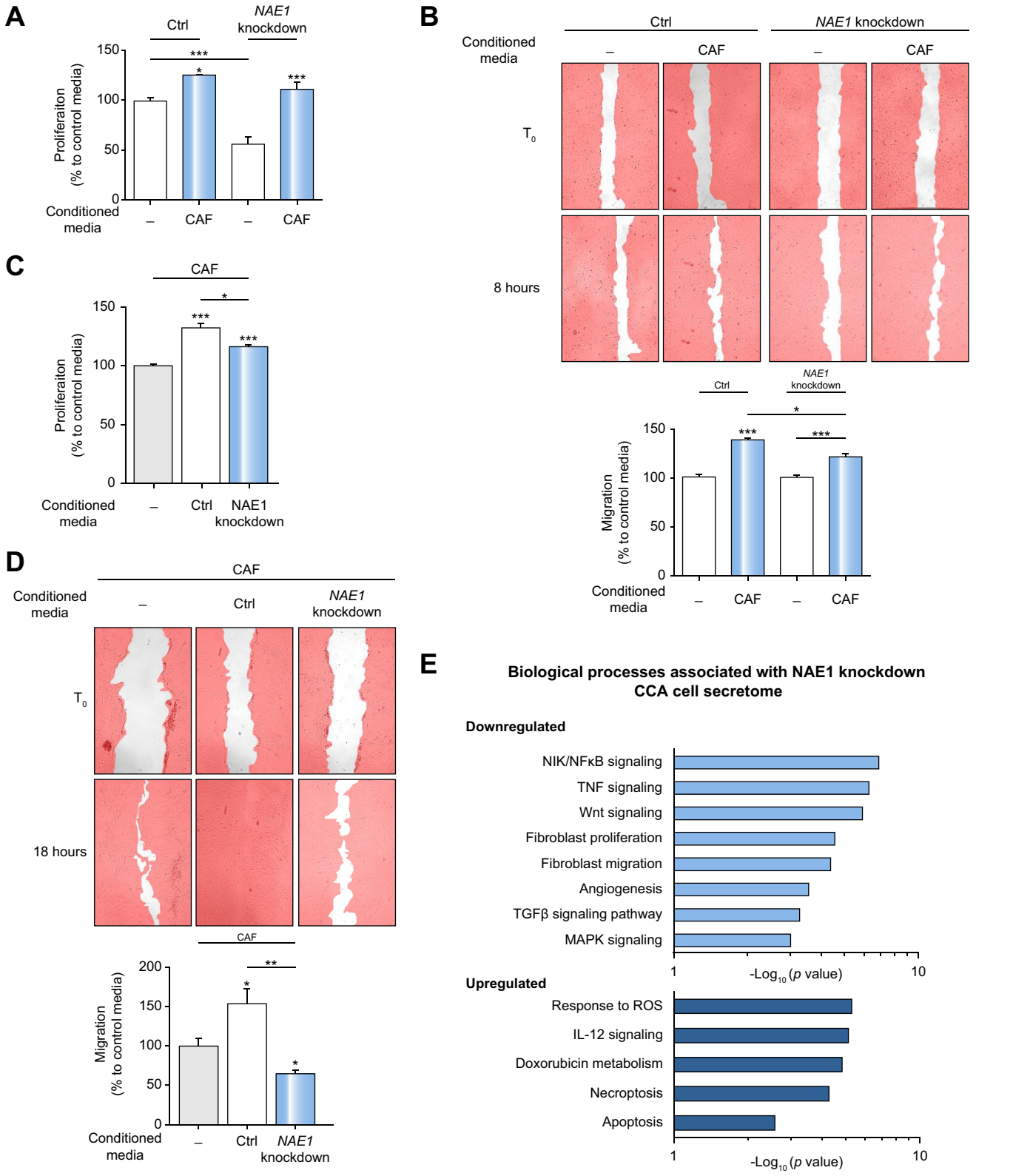

Fig. 7. NEDDylation impairment in CCA cells alters the crosstalk with CAFs. (A) Proliferation and (B) migration of Ctrl and *NAE1*-knockdown cells in the presence or absence of CAF-derived culture media (n = 3). (C) Proliferation and (D) migration of CAFs in the presence of Ctrl or *NAE1*-knockdown CCA cell-derived media (n = 3). (E) GO analysis of the significantly differentially regulated proteins in *NAE1*-knockdown CCA cell-derived supernatant compared to Ctrl CCA cell-derived media (n = 3). *p <0.05, **p <0.01, ***p <0.001 (one-way ANOVA or Kruskal-Wallis tests). CAF, cancer-associated fibroblast; CCA, cholangiocarcinoma; Ctrl, control.

replication (*e.g.*, MCM1, POLD3) and cell secretion-related proteins (*e.g.*, CATB, LAMC2) were mainly downregulated in CRISPR/Cas9-*NAE1* CCA cells (Fig. S12E). Most of the proteins upregulated in CRISPR/Cas9-*NAE1* CCA cells that were associated with vesicle transport are involved in autophagy (*e.g.*, BAP31, SNX4) or assembly and activity of tight junctions (*e.g.*, MRP, CAPZA1). In this regard, defects in NEDDylation lead to the activation of autophagy (Fig. S12F), probably to compensate for the loss of ubiquitination and proteasome-mediated degrading capacity due to inhibited CRL activation.[9] Additionally, changes in tight junction assembly and activity could result in the observed disturbances of the migratory capacity of CRISPR/Cas9-NAE1 CCA cells (Fig. S12G).

CRISPR/Cas9-*NAE1* CCA cells injected subcutaneously in immunodeficient mice showed lower tumorigenic capacity than CRISPR/Cas9 control cells (Fig. 6G-J). Furthermore, constitutive *Nae1* heterozygosity in mice (*Nae1*$^{+/-}$) prevented the development of preneoplastic CCA lesions in the liver after intravenous administration of plasmids encoding the *NICD*/*AKT* oncogenes and a sleeping beauty transposase (Fig. 6K-M).

NAE1 regulates the secretome of CCA cells, which in turn impacts on the proliferative and migratory capacities of CAFs *in vitro*

Given the abundance of CAFs in CCA tumors, the differential *NAE1* expression observed between tumor epithelia and stroma in microdissected tumor samples from the Copenhagen cohort, and the downregulation of cell secretion-related proteins in *NAE1*-knockdown CCA cells, the role of protein NEDDylation in the crosstalk between CCA cells and CAFs, and its additional effect on CCA progression was studied. For this purpose, human CCA-derived CAFs were isolated and further characterized (Fig. S14A). As expected, CAF-derived conditioned media markedly enhanced the proliferation, 3D growth, and migration of CCA cells (Fig. S14B-D). Interestingly, CAF-derived media boosted proliferation and migration in the CRISPR control and *NAE1*-knockdown CCA cells (Fig. 7A,B). Proliferation was particularly increased in *NAE1*-knockdown CCA cells upon CAF-derived media incubation, reaching the proliferation rates of control CCA cells (Fig. 7A). However, even if CAF-derived culture media stimulated migration in both CRISPR control and *NAE1*-knockdown CCA cells, the latter migrated less (Fig. 7B). Besides, the effect of CRISPR/Cas9-*NAE1* in CCA cells was evaluated on CAF proliferative capacity; we observed that control CCA cell-derived media increased CAF proliferation to a greater extent than that from *NAE1*-knockdown CCA cells (Fig. 7C). Moreover, NEDDylation inhibition in CCA cells affected CAF migration. Thus, CCA control cell-derived culture media augmented the baseline migratory capacity of CAFs, whereas conditional media derived from *NAE1*-knockdown CCA cells reduced CAF migration (Fig. 7D). Importantly, pevonedistat reduced CAF viability *per se*, highlighting the relevance of the NEDDylation pathway in stromal cells (Fig. S15).

Proteomic analysis of the secreted proteins in control and *NAE1*-knockdown CCA cells identified 213 differentially expressed proteins (Fig. S16). Among them, 110 proteins (51.6%) were upregulated (red) and 103 (48.4%) downregulated (blue) in *NAE1*-knockdown CCA cells compared to controls (Fig. S16). GO analysis revealed that the downregulated proteins in the secretome of CRISPR/Cas9-*NAE1* CCA cells were involved in fibroblast proliferation (*e.g.*, HMGA1, HMGA2), fibroblast migration (*e.g.*, COL6A1, FAM3C), angiogenesis (*e.g.*, ANXA2, AGRN), as well as with different pro-tumorigenic signaling networks, including NIK/NF-κB, TNF, Wnt, TGFβ, and MAPK pathways (Fig. 7E). On the other hand, proteins found upregulated in the secretome of CRISPR/Cas9-*NAE1* CCA cells are involved in reactive oxygen species response (*e.g.*, PRDX1), IL-12 signaling, necroptosis (*e.g.*, VCP) and apoptosis (*e.g.*, HMGB1) (Fig. 7E).

Discussion

Our study provides strong evidence that the expression levels of core NEDDylation pathway components are upregulated in human CCA tissue and cells compared to respective controls. The relevance of these findings is supported by the presence of elevated levels of NEDD8-conjugated proteins in CCA tumor epithelia and cell lines, which promote cholangiocarcinogenesis *in vitro* and *in vivo*. The increased levels of NEDDylated proteins seems to be a generalized and central event during cholangiocarcinogenesis, as it was found in CCA tumors from 5 independent international cohorts of patients regardless of the underlying driver mutations, as well as in 5 CCA cell lines compared to respective controls. These data are consistent with previous findings showing increased levels of some NEDDylation pathway components by IHC in human iCCA tumors.[11]

In an attempt to block the NEDDylation pathway, pevonedistat was developed as a first-in-class pharmacological inhibitor selectively targeting NAE.[8] Consistently, immunoblotting assays demonstrated a drastic reduction of NEDDylated protein levels in both CCA cell lines and NHCs following pevonedistat incubation. Besides, pevonedistat increased DNA damage, cell cycle arrest, apoptosis, and impaired proliferation and colony formation, ultimately reducing CCA tumorigenicity. In subcutaneous and orthotopic mouse models with human CCA cells, tumor growth was markedly inhibited by pevonedistat, highlighting a potential clinical value. Immunoprecipitation of NEDD8-conjugated proteins identified increased levels of multiple NEDDylated proteins in CCA cells compared to NHCs. For instance, the NEDDylated levels of cullins were found increased, probably as a reflection of their increased baseline protein expression in CCA cells compared to NHCs. Cullin NEDDylation results in CRL activation, which enhances ubiquitination of CRL substrates tagging them for proteasomal degradation. Hence, pharmacological inhibition of NEDDylation results in accumulation of CRL substrates.[8,12–14] Herein, we demonstrated that pevonedistat led to CDT1 and ORC1 accumulation and induced DNA damage. Thus, NEDDylation inhibition might activate the DNA damage G_2/M checkpoint, leading to the reported cell cycle arrest at G_2/M, attenuating the hyperproliferative capacity of CCA cells and concomitantly triggering apoptosis. Additionally, NEDDylation has been observed to be indispensable for DNA nucleotide excision repair and non-homologous end joining, suggesting that pevonedistat could impair these processes, and favor the accumulation of unrepaired DNA damage,[15] ultimately triggering CCA cell apoptosis. Furthermore, the tumor suppressors p21, p27 and WEE1, established substrates of CRLs,[12,14] were found to accumulate with pevonedistat. On the other hand, NEDDylated CDK1 levels were found increased in CCA cells. To our knowledge, this is the first evidence of CDK1 being a substrate for NEDD8. CDK1 and Cyclin B1 constitute an important complex that regulates G_2/M transition during cell cycle progression.[16] However, WEE1-mediated phosphorylation of CDK1 in Tyr15 prevents mitotic entry in response to DNA damage.[16] Interestingly, pevonedistat induced

DNA damage and accumulation of WEE1, and a consequent rise in phosphorylated CDK1 levels in CCA cells. These, together with the observed accumulation of Cyclin B1, seem to be involved in the previously described pevonedistat induction of G_2/M cell cycle arrest.

The first-line treatment for advanced CCA is the combination of GemCis, although it is considered merely palliative due to the presence and/or acquisition of mechanisms of chemoresistance.[1] Cisplatin predominantly causes single-strand breaks (99%), whereas inter-strand breaks are scarce (1%).[17] Hence, tumor cells treated with cisplatin can evolve and develop adaptive DNA repair mechanisms to survive.[1] Our results corroborate previous studies indicating that pevonedistat induces unrepairable DNA damage[18] that could prevent the development of adaptive mechanisms and, thus, the appearance of chemoresistance. Importantly, we demonstrated an augmented efficacy of the triple combination of GemCis and pevonedistat in CCA cells compared to GemCis or pevonedistat alone. Hence, pevonedistat can cooperate with cisplatin to induce DNA damage,[19] and therefore, increase CCA cell sensitivity to GemCis.

Aiming to further study the implications of NEDDylation in CCA and in order to confirm the anti-tumor capacity of pevonedistat, *NAE1*-knockdown cells were generated using the CRISPR/Cas9 methodology, and these were able to recapitulate most of the effects observed with pevonedistat *in vitro* and *in vivo*. Furthermore, *NAE1*-deficient CCA cells were characterized by downregulation of stemness markers and were incapable of forming spheroids, supporting our initial data where less-differentiated CCA tumors presented upregulated *NAE1* expression levels compared to well-differentiated ones. On the other hand, *Nae1*$^{+/-}$ mice, harboring impaired NEDDylation, seemed to be protected against the development of CCA preneoplastic lesions, supporting the role of this pathway in CCA origin and progression.

The crosstalk between tumor epithelia and stroma is of utmost importance in cancer. CCA presents an extensive TME, and its interaction regulates most cancer hallmarks. We have corroborated that CAF-derived media enhances CCA cell proliferation and migration.[20] Notably, pevonedistat was able to reduce CAF viability *per se*, indicating the relevance of NEDDylation in the TME. Focusing on CCA-TME interactions in the context of NEDDylation, differences between the secretome of CRISPR/Cas9 control and *NAE1*-knockdown CCA cells were analyzed. Significant differences were particularly observed in proteins related to fibroblast activation, proliferation, and migration. A reduced number of proteins associated with CAF activation and recruitment (HMGA1, HMGA2, and COL6A1, among others) were identified in the secretome of *NAE1*-knockdown CCA cells and could be involved in the reduction in CAF proliferation and migration detected after incubating CAFs with *NAE1*-knockdown cell-derived media. Furthermore, a downregulation of proteins related to angiogenesis was identified in the *NAE1*-deficient CCA cell secretome. On the other hand, the pro-tumorigenic effects of the secretome of CAFs seem to be independent of the NEDDylation status of CCA cells, as similar proliferation and migration results were obtained in CRISPR/Cas9 control and CRISPR/Cas9-*NAE1* CCA cells.

Overall, this study unravels the crucial role of the NEDDylation of proteins in cholangiocarcinogenesis and demonstrates the importance of the NEDDyation status of cancer cells in their crosstalk with CAFs, pointing to the role of aberrant protein NEDDylation not only in the behavior of the tumor or TME cells themselves, but also in their interaction. Furthermore, targeting the NEDDylation pathway with pevonedistat appears to be an attractive strategy to tackle CCA. Pevonedistat is safe and has been approved by the U.S. Food and Drug Administration for the treatment of patients with higher-risk myelodysplastic syndrome. Moreover, pevonedistat is currently being investigated in 26 clinical trials for different cancers and 7 additional ones have been completed (www.clinicaltrials.gov). Altogether, our data support the potential of pevonedistat (either alone or in combination) for the treatment of patients with CCA, which warrants further investigation.

Abbreviations

BAK, BCL2 agonist/killer; BAX, BCL2 associated X; BilIN, biliary intra-epithelial neoplasia; BIM, BCL2 like 11; CAFs, cancer-associated fibroblasts; CCA, cholangiocarcinoma; CDK1, cyclin-dependent kinase 1; CDT1, chromatin licensing and DNA replication factor 1; Cis, cisplatin; CRL, cullin RING ligase; CUL, cullin; EGF, epidermal growth factor; Gem, gemcitabine; GO, gene ontology; iCCA, intrahepatic cholangiocarcinoma; IDH, isocitrate dehydrogenase; IHC, immunohistochemistry; IL-6, interleukin 6; IP, immunoprecipitation; NAE1, NEDD8-activating enzyme E1; NEDD8, neural precursor cell expressed, developmentally down-regulated 8; NHCs, normal human cholangiocytes; NICD1, notch intracellular domain 1; ORC1, origin recognition center 1; PCNA, proliferating cell nuclear antigen; PDGF, platelet-derived growth factor; p-H2AX, phosphorylated-histone H2A family member X; PTMs, post-translational modifications; SL, surrounding liver; TCGA, The Cancer Genome Atlas; TIGER-LC, The Thailand Initiative in Genomics and Expression Research; TME, tumor microenvironment; UBE2F, ubiquitin-conjugating enzyme E2F; UBE2M, ubiquitin-conjugating enzyme E2M; UBA3, NEDD8-activating enzyme E1 catalytic subunit; VEGF, vascular endothelial growth factor.

Financial support

Spanish Carlos III Health Institute (ISCIII) [JMB (FIS PI21/00922, PI18/01075 and Miguel Servet CPII19/00008); MJP (FIS, PI17/00022, PI20/00186); PMR (Sara Borrell CD19/00254); JJGM (PI19/00819); RIRM (FIS PI20/00189); JMB and PA (PMP21/00080)] cofinanced by "*Fondo Europeo de Desarrollo Regional*" (FEDER); "*Ministerio de Ciencia, Innovación y Universidades*" (MICINN to MLM-C: PID2020-117116RB-I00), Spain; Spanish Ministry of Economy and Competitiveness (MINECO: "*Ramón y Cajal*" Program RYC-2015-17755 to MJP and RYC2018-024475-1 to MGF-B, and FPU 19/03327 to IO); CIBERehd (ISCIII): JMB, PMR, MJP, MA, FE, MLM-C, MAA, MGF-B, RIRM, JJGM, PA, and LB, Spain; Spanish Ministry of Science and Innovation (SAF2017-88933-R, PID2020-120387RB-I00 to MGF-B); "*Diputación Foral Gipuzkoa*" (2020-CIEN-000067-01 and 2021-CIEN-000029-04-01 to PMR), Spain; Department of Health of the Basque Country (2019111024 to MJP, 2017111010 to JMB, 2020111077 and 2021111021 to JMB and PA), "*Euskadi RIS3*" (2019222054, 2020333010, 2021333003 to JMB), BIOEF (Basque Foundation for Innovation and Health Research: EiTB Maratoia BIO15/CA/016/BD to JMB, MLM-C, MA), and Elkartek (KK-2020/00008 to JMB and MLM-C), Spain; La Caixa Scientific Foundation (JMB, MLM-C and REC: HR17-00601), Spain; "*Fundación Científica de la Asociación Española Contra el Cáncer*" (AECC Scientific Foundation: "Rare cancers call 2017" to JMB, MLM-C, MAA, JJGM, and "AECC Lab call 2020" to MGF-B), Spain; AMMF-The Cholangiocarcinoma Charity (EU/2019/

AMMFt/001, to JMB and PMR), United Kingdom; "*Centro Internacional sobre el Envejecimiento*" (OLD-HEPAMARKER, 0348-CIE-6-E, to RIRM, JJGM and REC), Spain; "*Junta de Castilla y León*" (SA074P20, to JJGM), Spain; "*Fundació la Marató TV3*" (201916-31, to JJGM), Spain; "*Fundação para a Ciência e a Tecnologia*" (FCT) (PTDC/MED-PAT/31882/2017, to REC), Portugal. PO and IO by the Basque Government (PRE_2016_1_0269 and PRE_2019_1_0197), PYL-L by the European Association for the Study of the Liver (EASL; Sheila Sherlock Award 2017) and FJC-C by the University of the Basque Country (MARSA21/17). We thank MINECO for the Severo Ochoa Excellence Accreditation to CIC bioGUNE (SEV-2016-0644). The funding sources had no involvement in study design, data collection and analysis, decision to publish, or preparation of the article.

Conflict of interest

Authors disclose no conflict of interest related to this manuscript.

Please refer to the accompanying ICMJE disclosure forms for further details.

Authors' contributions

PO, PYL-L, MGF-B, MC, MA, CJO, FJC-C, IO, RIRM, JJGM, DFC, MLM-C, MAA, PA, DFC, ME, LF, REC, FE, JBA, LB, PMR, MJP, JMB: study concept and design, analysis and interpretation of data, drafting of the manuscript. PO, PYL-L, MGF-B, MA, CJO, PMR, FJC-C, IO, DFC, JMB: acquisition of data. PO, MA, CJO, FJC-C, IO, PMR, JMB: statistical analysis. JJGM, RIRM, MLM-C, MAA, LB, MJP, JMB: obtained funding.

Data availability statement

Research data is confidential except for the proteomics data, which have been deposited and are available in PRIDE repository with the dataset identifiers PXD021139 and PXD021140.

Acknowledgements

This article is based upon work from the COST Action CA18122 European Cholangiocarcinoma Network supported by COST (European Cooperation in Science and Technology: www.cost.eu).

Supplementary data

Supplementary data to this article can be found online at https://doi.org/10.1016/j.jhep.2022.02.007.

References

Author names in bold designate shared co-first authorship

[1] Banales JM, Marin JJG, Lamarca A, Rodrigues PM, Khan SA, Roberts LR, et al. Cholangiocarcinoma 2020: the next horizon in mechanisms and management. Nat Rev Gastroenterol Hepatol 2020;17:557–588. https://doi.org/10.1038/s41575-020-0310-z.

[2] **Rodrigues PM**, **Olaizola P**, Paiva NA, Olaizola I, Agirre-Lizaso A, Landa A, et al. Pathogenesis of cholangiocarcinoma. Annu Rev Pathol Mech Dis 2021;16:433–463. https://doi.org/10.1146/annurev-pathol-030220-020455.

[3] Affo S, Nair A, Brundu F, Ravichandra A, Bhattacharjee S, Matsuda M, et al. Promotion of cholangiocarcinoma growth by diverse cancer-associated fibroblast subpopulations. Cancer Cell 2021. https://doi.org/10.1016/j.ccell.2021.03.012.

[4] Deribe YL, Pawson T, Dikic I. Post-translational modifications in signal integration. Nat Struct Mol Biol 2010;17:666–672. https://doi.org/10.1038/nsmb.1842.

[5] Yavuz AS, Sözer NB, Sezerman OU. Prediction of neddylation sites from protein sequences and sequence-derived properties. BMC Bioinformatics 2015;16. https://doi.org/10.1186/1471-2105-16-S18-S9.

[6] Delgado TC, Barbier-Torres L, Zubiete-Franco I, Lopitz-Otsoa F, Varela-Rey M, Fernández-Ramos D, et al. Neddylation, a novel paradigm in liver cancer. Transl Gastroenterol Hepatol 2018;3. https://doi.org/10.21037/tgh.2018.06.05.

[7] **Lee-Law PY**, **Olaizola P**, Caballero-Camino FJ, Izquierdo-Sanchez L, Rodrigues PM, Perugorria MJ, et al. Inhibition of NAE-dependent protein hyper-NEDDylation in cystic cholangiocytes halts cystogenesis in experimental models of polycystic liver disease. United Eur Gastroenterol J 2021;9:848–859. https://doi.org/10.1002/ueg2.12126.

[8] Soucy TA, Smith PG, Milhollen MA, Berger AJ, Gavin JM, Adhikari S, et al. An inhibitor of NEDD8-activating enzyme as a new approach to treat cancer. Nature 2009;458:732–736. https://doi.org/10.1038/nature07884.

[9] **Lee-Law PY**, **Olaizola P**, Caballero-Camino FJ, Izquierdo-Sanchez L, Rodrigues PM, Santos-Laso A, et al. Targeting UBC9-mediated protein hyper-SUMOylation in cystic cholangiocytes halts polycystic liver disease in experimental models. J Hepatol 2021;74:394–406. https://doi.org/10.1016/j.jhep.2020.09.010.

[10] Li L, Che L, Tharp KM, Park HM, Pilo MG, Cao D, et al. Differential requirement for de novo lipogenesis in cholangiocarcinoma and hepatocellular carcinoma of mice and humans. Hepatology 2016;63:1900–1913. https://doi.org/10.1002/HEP.28508.

[11] Gao Q, Yu GY, Shi JY, Li LH, Zhang WJ, Wang ZC, et al. Neddylation pathway is up-regulated in human intrahepatic cholangiocarcinoma and serves as a potential therapeutic target. Oncotarget 2014;5:7820–7832. https://doi.org/10.18632/oncotarget.2309.

[12] Soucy TA, Dick LR, Smith PG, Milhollen MA, Brownell JE. The NEDD8 conjugation pathway and its relevance in cancer biology and therapy. Genes Cancer 2010;1:708–716. https://doi.org/10.1177/1947601910382898.

[13] Chiba T, Tanaka K. Cullin-based ubiquitin ligase and its control by NEDD8-conjugating system. Curr Protein Pept Sci 2005;5:177–184. https://doi.org/10.2174/1389203043379783.

[14] Petroski MD, Deshaies RJ. Function and regulation of cullin-RING ubiquitin ligases. Nat Rev Mol Cell Biol 2005;6:9–20. https://doi.org/10.1038/nrm1547.

[15] Luo Y, Su Y, Rao F. Role of NEDD8 and neddylation dynamics in DNA damage response. Genome Instab Dis 2021;2:139–149. https://doi.org/10.1007/S42764-021-00044-Z. 23 2021.

[16] Rhind N, Russell P. Tyrosine phosphorylation of Cdc2 is required for the replication checkpoint in Schizosaccharomyces pombe. Mol Cell Biol 1998;18:3782–3787. https://doi.org/10.1128/mcb.18.7.3782.

[17] Lippard SJ. New chemistry of an old molecule: cis-[Pt(NH3) 2Cl2]. Science (80) 1982;218:1075–1082. https://doi.org/10.1126/science.6890712.

[18] Brown JS, Jackson SP. Ubiquitylation, neddylation and the DNA damage response. Open Biol 2015;5. https://doi.org/10.1098/RSOB.150018.

[19] Nawrocki ST, Kelly KR, Smith PG, Espitia CM, Possemato A, Beausoleil SA, et al. Disrupting protein NEDDylation with MLN4924 is a novel strategy to target cisplatin resistance in ovarian cancer. Clin Cancer Res 2013;19:3577–3590. https://doi.org/10.1158/1078-0432.CCR-12-3212.

[20] Chuaysri C, Thuwajit P, Paupairoj A, Chau-In S, Suthiphongchai T, Thuwajit C. Alpha-smooth muscle actin-positive fibroblasts promote biliary cell proliferation and correlate with poor survival in cholangiocarcinoma. Oncol Rep 2009;21:957–969. https://doi.org/10.3892/or_00000309.